

# Self-consistent model for ambipolar tunnelling in quantum-well systems

C Presilla, V Emiliani and A Frova

Dipartimento di Fisica, Università di Roma 'La Sapienza', Piazzale A Moro 2, Roma 00185, Italy

Received 14 October 1994, in final form 17 January 1995, accepted for publication 30 January 1995

**Abstract.** We present a self-consistent approach to describe ambipolar tunnelling in asymmetrical double quantum wells under steady-state excitation and extend the results to the case of tunnelling from a near-surface quantum well to surface states. The results of the model compare very well with the behaviour observed in photoluminescence experiments in InGaAs/InP asymmetric double quantum wells and in near-surface AlGaAs/GaAs single quantum wells.

## 1. Introduction

The tunnelling of electrons and holes in quasi-two-dimensional semiconductor heterostructures is of great interest both for its physical interest—it is one of the most important quantum-mechanical effects observed in low-dimensional structures—and for its role in several nanometric devices and applications. Much work has been done concerning tunnelling in symmetrical and asymmetrical double quantum wells (ADQW).

Tunnelling from a quantum well (QW) to surface states, in contrast, has received little attention, despite the great importance of gaining control over this mechanism. For a quantum well built in the neighbourhood of an unpassivated surface, an extra non-radiative recombination channel becomes available to electrons and holes if they can tunnel to surface states, with a consequent loss in emission efficiency from the quantum well. The importance of this effect has been demonstrated experimentally in recent papers and its dependence on surface barrier thickness investigated [1–4].

In the interpretation of the experimental results, both tunnelling to surface states and tunnelling between ADQW, a problem arises. Although in some cases hole-tunnelling rates can be comparable to the electronic ones, e.g. when heavy holes in one well move to a light hole state in the other well [5], direct-gap III–V semiconductors have in general rather different tunnelling probabilities for electrons and holes due to the different effective masses [6, 7]. The difference in tunnelling probability for the two carriers causes a dipole electric field across the tunnelling barrier to develop [8–11], so as to induce—via the quantum-confined Stark effect [12]—a peak shift of the excitonic recombination, and to affect the tunnelling probabilities towards an ambipolar regime, with equal tunnelling currents for electrons and holes.

The appearance of an electric field due to the spatial separation of electrons and holes in ADQW systems has already been discussed theoretically [13] in the framework of exciton tunnelling under impulsive excitation. In this paper we study the tunnelling of unpaired electrons and holes both in ADQW and in near-surface QW systems under steady-state excitation. Unlike the case of impulsive excitation, not discussed in this paper, the ambipolar regime is shown to be reached in this case for any excitation intensity. The consequently modified tunnelling properties are successfully compared with available experiments, i.e. the dependence of the emission efficiency ratio in ADQW systems on the excitation power and the tunnelling barrier width [9], the dependence of the tunnelling current on the barrier thickness [1] and the dependence of the Stark shift on the excitation level in a near-surface QW [8].

## 2. Tunnelling between two asymmetric quantum wells

Here we describe the steady-state photoluminescence from two coupled asymmetric quantum wells under constant irradiation. The charges photogenerated inside the wells relax almost instantaneously with respect to the other relevant time scales to the lowest band of the respective well and fill it according to the Pauli principle. Electron-hole interaction leads to exciton formation. Tunnelling between the two wells is essentially restricted to unpaired electrons and holes when the tunnelling process is a small perturbation for the nearly uncoupled wells: as a matter of fact, the tunnelling current densities correspond to a first-order process for unpaired electrons and holes and to a second-order process for excitons. On the other hand photoluminescence is restricted to only excitonic recombination.

Let  $a_1$  and  $a_2$  be the widths of the two quantum wells and  $b$  the width of the barrier between them. We suppose

$a_1 > a_2$  so that the bottom of the e1 and hh1 bands of well 2,  $E_{e1}^{(2)}$  and  $E_{hh1}^{(2)}$ , are higher in energy than those of well 1,  $E_{e1}^{(1)}$  and  $E_{hh1}^{(1)}$ . Let  $G_1$  and  $G_2$  be the generation current densities of electron-hole pairs in the two wells. If  $n_i$  and  $p_i$  are the steady-state concentrations (number of particles per unit area) of electrons and holes in the well  $i = 1, 2$ , the following rate equations hold:

$$0 = G_1 + J_e - \lambda_1 n_1 p_1 \quad (1a)$$

$$0 = G_1 + J_h - \lambda_1 n_1 p_1 \quad (1b)$$

$$0 = G_2 - J_e - \lambda_2 n_2 p_2 \quad (1c)$$

$$0 = G_2 - J_h - \lambda_2 n_2 p_2 \quad (1d)$$

$$0 = \lambda_1 n_1 p_1 - I_1 \quad (1e)$$

$$0 = \lambda_2 n_2 p_2 - I_2. \quad (1f)$$

The first two pairs of equations are the rate equations for the concentrations of unpaired electrons and holes in wells 1 and 2 respectively, and contain, in that order, the photogeneration and tunnelling current densities of the unpaired charges and the generation current density of excitons. The last two equations are the rate equations for the exciton concentrations in wells 1 and 2 and contain the photoluminescence current densities  $I_1$  and  $I_2$ , which are the quantities we want to evaluate and compare with experimental results.

The generation current density of excitons in well  $i$  is assumed to be proportional to the concentrations of the unpaired charges in the same well,  $\lambda_i n_i p_i$ , where  $\lambda_i$  is the bimolecular exciton formation coefficient and is possibly dependent on the well size [14].

A little more complicated analysis is needed for the tunnelling current densities  $J_e$  and  $J_h$ . Transfer of electrons (holes) from the narrower well to the larger one occurs in a non-coherent two-step process. Quantum coherent tunnelling of electrons (holes) from an occupied state of the e1 (hh1) band of well 2 to an equal-energy empty state of the e1 (hh1) band of well 1 is followed by thermalization towards the lower energy states of well 1. When the barrier width  $b$  is not too small, which is also the range of validity of the above rate equations, the quantum coherent tunnelling process characterized by a time growing exponentially with  $b$  gets much slower than the thermalization process in well 1 ( $\lesssim 1$  ps [15]) and this last can be neglected.

The current densities for quantum coherent tunnelling are approximately proportional to the charge concentrations in well 2, and the proportionality factor, namely the tunnelling rate, is quite different for electrons and holes due to their different effective masses. Therefore, in a steady-state situation when  $J_e = J_h$ , the concentrations of electrons and holes in each single well must be different and an electric field gets established in the barrier between the two wells. Moreover the electric field modifies the electron and hole tunnelling rates. The direction of the field is simply understood from the values of the tunnelling rates at zero field. As the electron tunnelling rate is expected in this case to be much greater than the hole tunnelling rate, electrons accumulate at well 1 and in a steady-state situation

$n_1 > p_1$ . The electric field is directed from well 2 to well 1 and its value is given by

$$F = \frac{en}{\epsilon_0 \epsilon_r} \quad (2)$$

where  $n = n_1 - p_1 = p_2 - n_2$  and  $\epsilon_r$  is the permittivity of the barrier material.

The tunnelling current densities depend on the electric field  $F$  through the dependence of the charge concentrations on  $F$  as well as through the dependence of the tunnelling rate on the energy shift between the bands of the two wells induced by  $F$ . Assuming that the electric field is completely shielded inside the wells, this energy shift amounts to  $eFb$ . For a given value of  $F$ , the tunnelling current densities can be evaluated within perturbation theory in the case of a barrier that is not too thin. To first order the transition rate induced by a constant perturbation  $V$  between initial and final states continuously distributed in energy with densities  $dN_i/d\epsilon$  and  $dN_f/d\epsilon$ , respectively, is [16]

$$\begin{aligned} & \int \int \frac{2\pi}{\hbar} |\langle i, \epsilon | V | f, \epsilon' \rangle|^2 \delta(\epsilon - \epsilon') dN_f(\epsilon') dN_i(\epsilon) \\ &= \int \frac{2\pi}{\hbar} |\langle i, \epsilon | V | f, \epsilon \rangle|^2 \frac{dN_f}{d\epsilon}(\epsilon) \frac{dN_i}{d\epsilon}(\epsilon) d\epsilon. \end{aligned} \quad (3)$$

This formula, when applied to the electron and hole states of the two uncoupled wells and divided by the transverse area  $A$  of the heterostructure, gives the following expressions for the tunnelling current densities:

$$\begin{aligned} J_e &= \frac{1}{A} \int_0^\infty \frac{2\pi}{\hbar} |\langle \Phi_\epsilon^{(1)} | V_e | \Phi_\epsilon^{(2)} \rangle|^2 A v_e^{(1)} \\ &\quad \times \left[ 1 - f \left( \frac{\epsilon - \epsilon_F^{(1)}}{k_B T} \right) \right] A v_e^{(2)} f \left( \frac{\epsilon - \epsilon_F^{(2)}}{k_B T} \right) d\epsilon \end{aligned} \quad (4)$$

$$\begin{aligned} J_h &= \frac{1}{A} \int_0^\infty \frac{2\pi}{\hbar} |\langle \Phi_\epsilon^{(1)} | V_h | \Phi_\epsilon^{(2)} \rangle|^2 A v_h^{(1)} \\ &\quad \times \left[ 1 - f \left( \frac{\epsilon - \epsilon_F^{(1)}}{k_B T} \right) \right] A v_h^{(2)} f \left( \frac{\epsilon - \epsilon_F^{(2)}}{k_B T} \right) d\epsilon. \end{aligned} \quad (5)$$

The integration takes into account the transitions from all the occupied states in the e1 (hh1) band of well 2 (initial states) to the empty states in the e1 (hh1) band of well 1 (final states) at the same energy  $\epsilon$  measured from the bottom of the e1 (hh1) band of well 2. The densities of the available initial (final) states are obtained by multiplying the number of states per unit energy  $A v^{(2)}$  ( $A v^{(1)}$ ) by the appropriate occupation probability. Here  $v_e^{(i)} = m_e^{(i)}/\pi\hbar^2$  ( $v_h^{(i)} = m_h^{(i)}/\pi\hbar^2$ ),  $i = 1, 2$ , are the densities per unit area and unit energy of a two-dimensional ideal gas of fermions with mass  $m_e^{(i)}$  ( $m_h^{(i)}$ ) and  $f(x) = 1/[\exp(x) + 1]$  is the Fermi function. The Fermi energies for electrons (holes) are related to the concentrations in the corresponding well:  $\epsilon_F^{(1)} = \pi\hbar^2 n_1/m_e^{(1)} + E_{e1}^{(1)} + eFb - E_{e1}^{(2)}$  and  $\epsilon_F^{(2)} = \pi\hbar^2 n_2/m_e^{(2)}$  ( $\epsilon_F^{(1)} = \pi\hbar^2 p_1/m_h^{(1)} + E_{hh1}^{(1)} - eFb - E_{hh1}^{(2)}$  and  $\epsilon_F^{(2)} = \pi\hbar^2 p_2/m_h^{(2)}$ ). Finally, the perturbation potential  $V_e$  ( $V_h$ ) is the potential of the heterostructure ( $b$  finite) coupling the electron (hole) states evaluated by considering the wells as uncoupled ( $b$  infinite). Due to the exponentially vanishing tails of the electron (hole) wavefunctions, the

relevant contribution to the matrix elements comes only from the barrier region between the two wells [16]. In this region the potential  $V_e$  ( $V_h$ ) has a magnitude of the order of the conduction (valence) band offset  $\Delta E_c$  ( $\Delta E_v$ ). More accurate expressions for  $V_e$  ( $V_h$ ), e.g. taking into account the distortion due to the electric field, have little influence on the final result and will be neglected. Explicit expressions for  $\Phi$  of the electron and hole states and analytical evaluation of the matrix elements are given in appendix A.

The formulas for the tunnelling current densities can be simplified by noting that, due to the exponentially large difference between electron and hole tunnelling rates, we expect  $n_2 \ll n_1$ . As a consequence, the electron Fermi energy  $\epsilon_F^{(2)}$ , i.e. the effective region of integration in equation (4), is very small. By approximating all factors to be integrated in (4) except the Fermi function in well 2 by their value at  $\epsilon = 0$  (the bottom of the e1 band of well 2) we get  $J_e = n_2/\tau_e$ , where  $n_2 = \int v_e^{(2)} f[(\epsilon - \epsilon_F^{(2)})/k_B T] d\epsilon$  and

$$\frac{1}{\tau_e} = \frac{2\pi}{\hbar} \left| \langle \Phi_0^{(1)} | V_e | \Phi_0^{(2)} \rangle \right|^2 A v_e^{(1)} f \left( \frac{\epsilon_F^{(1)}}{k_B T} \right). \quad (6)$$

In the case of holes we expect  $p_2 \gg p_1$  so that  $\epsilon_F^{(2)}$  is not small. However, in this case  $\epsilon_F^{(1)} < 0$  (now the zero of energy is the bottom of the hh1 band of well 2) and  $f[(\epsilon - \epsilon_F^{(1)})/k_B T] \simeq 0$ . Neglecting the smooth dependence of the matrix element on  $\epsilon$  in (5) we get  $J_h = p_2/\tau_h$  where  $p_2 = \int v_h^{(2)} f[(\epsilon - \epsilon_F^{(2)})/k_B T] d\epsilon$  and

$$\frac{1}{\tau_h} = \frac{2\pi}{\hbar} \left| \langle \Phi_0^{(1)} | V_h | \Phi_0^{(2)} \rangle \right|^2 A v_h^{(1)}. \quad (7)$$

Note that both the tunnelling rates  $1/\tau_e$  and  $1/\tau_h$  depend on the electric field through the matrix elements (see appendix A). In addition the electron tunnelling rate depends on  $F$  through the Fermi energy of well 1.

If we think that the electric field, i.e.  $n$ , and the tunnelling rates are known, we get the following solution for the initial set of rate equations:

$$n_2 = \sqrt{\left( \frac{n}{2} + \frac{1}{2\lambda_2\tau_e} \right)^2 + \frac{G_2}{\lambda_2}} - \left( \frac{n}{2} + \frac{1}{2\lambda_2\tau_e} \right) \quad (8a)$$

$$n_1 = \sqrt{\left( \frac{n}{2} \right)^2 + \frac{G_1}{\lambda_1} + \frac{n_2}{\lambda_1\tau_e} + \frac{n}{2}} \quad (8b)$$

$$p_1 = n_1 - n \quad (8c)$$

$$p_2 = n_2 + n. \quad (8d)$$

This result allows us to find the steady-state values of the electric field, of the charge concentrations and of the tunnelling rates by a recursive method. We proceed in the following manner. First of all we fix an electric field value corresponding to some negative electric charge concentration  $n$  in well 1. Then we evaluate the hole tunnelling rate and give a starting value to the electron tunnelling rate (for instance that obtained for  $n_1 = n$ ) so we can deduce some charge concentrations using equation (8).

From these concentrations we evaluate a new electron tunnelling rate using equation (6) and from that new charge concentrations. After a few iterations, the electron tunnelling rate and the charge concentrations converge to the solution corresponding to the value of the electric field fixed at the beginning. At this point we compare the values of the tunnelling current densities. If  $J_e > J_h$  the electric field is increased; if  $J_e < J_h$  the electric field is decreased. The procedure is repeated until the steady-state condition  $J_e = J_h$  is reached. Note that the existence of the ambipolar regime does not rely upon the value of the excitation intensity, i.e.  $G_1$  and  $G_2$ . However, the value of the electric field established in the steady state strongly depends on the excitation intensity.

We illustrate the behaviour of the model by considering a practical example close to the experimental situation investigated by Sauer *et al* [9]. We consider two  $\text{In}_{0.53}\text{Ga}_{0.47}\text{As}$  quantum wells embedded between  $\text{InP}$  barriers with  $a_1 = 100 \text{ \AA}$  and  $a_2 = 60 \text{ \AA}$ . We use the following material parameters at  $T = 4.2 \text{ K}$  [17]:  $\Delta E_c = 0.195 \text{ eV}$ ,  $\Delta E_v = 0.293 \text{ eV}$ ,  $m_e^{(1)} = m_e^{(2)} = 0.044 m$ ,  $m_h^{(1)} = m_h^{(2)} = 0.38 m$ ,  $m$  being the free electron mass, and  $\epsilon_r = 13.9$ . Moreover we put  $\lambda_1 = \lambda_2 = 6 \text{ cm}^2 \text{ s}^{-1}$  [14]. Since  $\alpha a_1, \alpha a_2 \ll 1$ , where  $\alpha$  is the optical absorption coefficient for the pump light, we take  $G_1/G_2 = a_1/a_2$  and  $G_2 = P/h\nu$  where  $P$  is the absorbed power density and  $h\nu = 2.41 \text{ eV}$  is the photon energy corresponding to  $514 \text{ nm}$  laser light. Note that the transverse area  $A$  shown in equations (6) and (7) cancels out with the  $A^{-1}$  from the squared matrix elements and is an irrelevant parameter.

In figure 1 we show the calculated photoluminescence intensity ratio  $I_1/I_2$  from the two wells as a function of the absorbed power density  $P$  for different values of the barrier width  $b$ . The self-consistent electric field  $F$  generated between the two wells in the same cases is shown in figure 2. When  $P$  is lower than a critical value, which depends on the barrier width, the photoluminescence intensity ratio  $I_1/I_2$  approximately decreases as  $P^{-1}$  and the electric field increases as  $P$ . When  $P$  reaches and exceeds the critical value an electric field of the order of  $3\text{--}4 \times 10^4 \text{ V cm}^{-1}$  becomes established, which slows down the tunnelling of electrons from well 2 to well 1 and enhances the photoluminescence from well 2. At very high absorbed power density the ratio  $I_1/I_2$  tends to the value  $G_1/G_2$  for two uncoupled wells. These results compare quite well with the experimental findings [9] if one assumes a 0.1% excitation efficiency.

A deeper understanding of the behaviour shown in figures 1 and 2 can be reached by an approximate solution of the self-consistent procedure described above. Let us first concentrate on the dependence of the electric field, i.e.  $n$ , on the absorbed power density  $P$ . In the steady state we have  $n_2/\tau_e = p_2/\tau_h$ , which combined with equations (8a) and (8d) gives

$$n = \frac{1}{2\lambda_2} \left( \frac{1}{\tau_e} - \frac{1}{\tau_h} \right) \left( \sqrt{1 + \frac{4\lambda_2\tau_e\tau_h}{h\nu} P} - 1 \right). \quad (9)$$

When  $P$  is not too high the second term in the square root

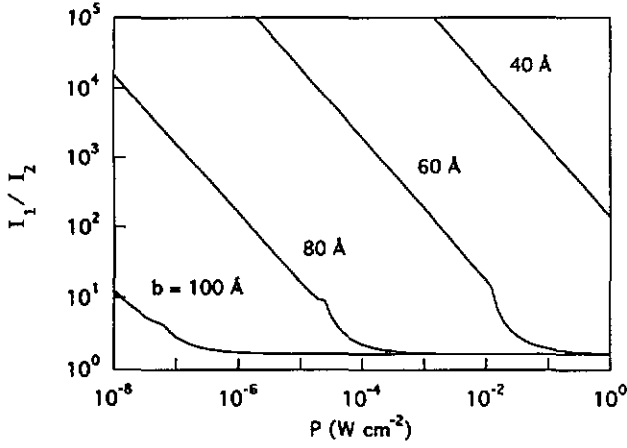


**Figure 1.** Calculated emission intensity ratio  $I_1/I_2$  from two coupled asymmetric wells versus absorbed power density  $P$  for various values of the barrier width  $b$ .

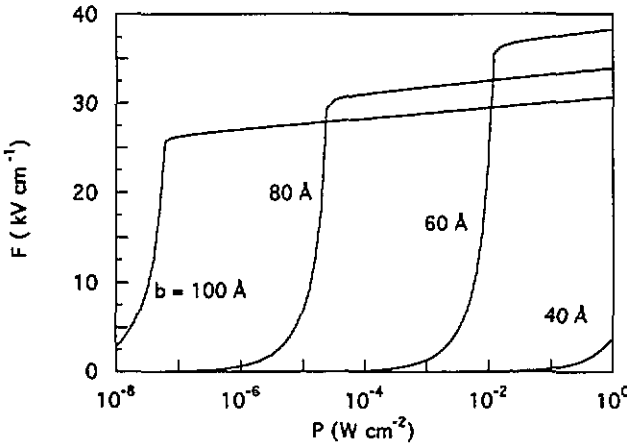


**Figure 2.** Calculated electric field  $F$  which becomes established between the two wells, in the same cases as figure 1.

is small and we get the simple self-consistent equation

$$n + \frac{\tau_e(n)}{h\nu} P = \frac{\tau_h}{h\nu} P. \quad (10)$$

In a first approximation the smooth dependence of the tunnelling rates on the electric field through the corresponding matrix elements can be neglected, so that  $\tau_h$  is constant while  $\tau_e$  still depends on  $n$  through the Fermi function. The argument of the Fermi function in equation (6) is negative until the alignment of the electron bands is achieved due to the electric field, i.e. in the region  $n \leq n_{crit}$  where  $e^2 b n_{crit} / \epsilon_0 \epsilon_r = E_{e1}^{(2)} - E_{e1}^{(1)}$ . In this range  $\tau_e$  is approximately constant and much smaller than  $\tau_h$ . On the other hand, for  $n > n_{crit}$  the electron tunnelling time increases exponentially with the dimensionless parameter  $eFb/k_B T$ , i.e. with  $n$ . The behaviour of  $\tau_e(n)$  imposes different solutions to equation (10) at different values of the absorbed power density. At low  $P$  we have  $\tau_e(n)P/h\nu \ll n$  and therefore  $n \simeq \tau_h P/h\nu$ . At high  $P$  we have  $\tau_e(n)P/h\nu \gg n$  and therefore  $n \simeq n_{crit}$  is constant. The critical value of the electric field is related to the critical value of the absorbed power density by  $P_{crit} \simeq h\nu n_{crit} / \tau_h$ . Since  $\tau_h$  increases exponentially with the barrier width  $b$ ,

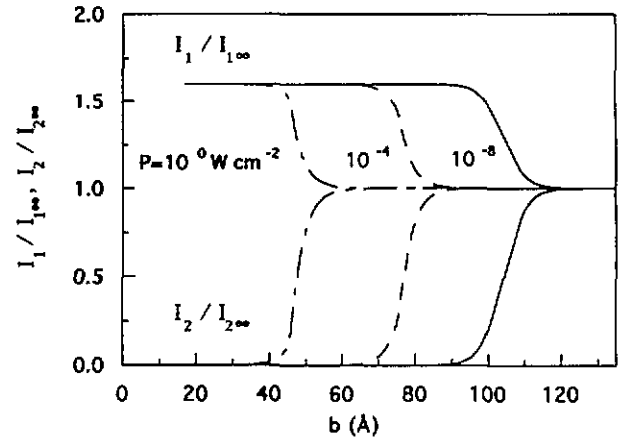


**Figure 3.** Calculated normalized photoluminescence intensities  $I_1/I_{1\infty}$  and  $I_2/I_{2\infty}$  versus barrier thickness  $b$  for different absorbed power densities  $P$ .  $I_{i\infty}$  is the photoluminescence intensity from well  $i$  in the limit  $b \rightarrow \infty$ .

$P_{crit}$  decreases exponentially with increasing  $b$  in agreement with figure 2.

The behaviour of  $n(P)$  allows us to understand also the features of figure 1. By approximating equation (8a) with  $n_2 \simeq G_2 \tau_e / (1 + n \lambda_2 \tau_e)$  we get

$$\frac{I_1}{I_2} = \frac{\lambda_1 n_1 (n_1 - n)}{\lambda_2 n_2 (n_2 + n)} \simeq \frac{1}{n \lambda_2 \tau_e} \left( 1 + \frac{G_1}{G_2} (1 + n \lambda_2 \tau_e) \right). \quad (11)$$

When  $P \ll P_{crit}$  the electron tunnelling time is almost constant,  $n \lambda_2 \tau_e \ll 1$  and the ratio  $I_1/I_2$  decreases as  $n^{-1}$ , i.e.  $P^{-1}$ . The behaviour of  $I_1/I_2$  changes drastically at the critical power  $P_{crit}$  due to the exponential change of  $\tau_e$ , and finally for  $n \lambda_2 \tau_e \gg 1$  the asymptotic value  $I_1/I_2 = G_1/G_2$  is obtained.

For the purpose of comparison with the following section, in figure 3 we show the behaviour of the calculated normalized photoluminescence intensities  $I_i/I_{i\infty}$ ,  $i = 1, 2$ , in the same ADQW of figures 1 and 2 as a function of the barrier width  $b$  and for different absorbed powers. The normalization  $I_{i\infty}$  is the photoluminescence current density for  $b \rightarrow \infty$ . The corresponding self-consistent electric field is shown in figure 4. The normalized photoluminescence intensity of well 2 (figure 3) vanishes at smaller  $b$  when the tunnelling current becomes higher. In this limit  $J_e \rightarrow G_2$ . At the same time the normalized photoluminescence intensity of well 1 tends to  $(G_1 + J_e)/G_1 = 1 + G_2/G_1$ . The self-consistent electric field (figure 4) gradually increases for decreasing  $b$ , until, in the tunnelling-dominated limit  $I_2/I_{2\infty} \rightarrow 0$ , it vanishes exponentially.

### 3. Tunnelling from a quantum well to surface states

The considerations developed in the previous sections can be extended to describe the case where a single quantum well is close to a surface. This is another situation where tunnelling is followed by recombination [1–4, 8]. Electron and hole bands of defect states localized at the surface play the role of the e1 and hh1 bands of the missing well. In a steady-state situation the system can still be described by

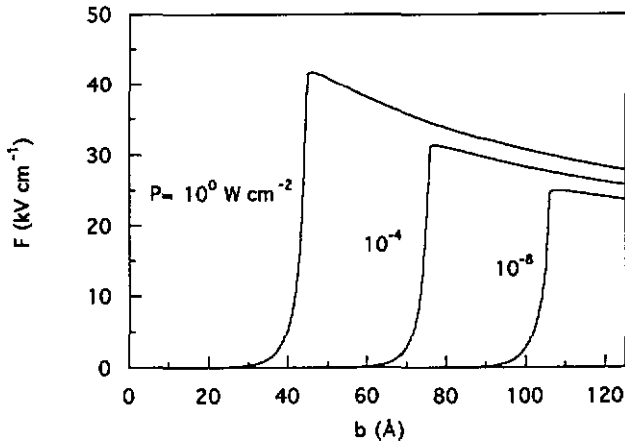


**Figure 4.** Calculated electric field  $F$  which becomes established between the two wells in the same cases as figure 3.

the rate equations (1) where the index 1 is associated with the surface and the index 2 with the well. Let  $n_1$  and  $p_1$  be the charge concentrations in the donor-like and acceptor-like surface bands. We can neglect the photogeneration of pairs at the surface so that  $G_1 = 0$ . Moreover  $\lambda_1 n_1 p_1 = I_1$  represents the non-radiative recombination current density at the surface. Since electrons and holes recombine (through a multiphonon process) very fast with respect to the other relevant time scales, one is allowed to take  $\lambda_1 \rightarrow \infty$ .

The tunnelling current densities from the occupied states of well 2 to the empty surface states 1 are still given by the general expressions (4) and (5). Now, however, the surface densities  $\nu_e^{(1)}$  and  $\nu_h^{(1)}$  are not constant in general. This implies the following definition for the corresponding Fermi energies:

$$\int_{E_{e1}^{(1)} + eFb - E_{e1}^{(2)}}^{\epsilon_F^{(1)}} \nu_e^{(1)}(\epsilon) d\epsilon = n_1 \quad (12)$$

for the donor-like band, and

$$\int_{E_{hh1}^{(1)} - eFb - E_{hh1}^{(2)}}^{\epsilon_F^{(1)}} \nu_h^{(1)}(\epsilon) d\epsilon = p_1 \quad (13)$$

for the acceptor-like band. As in the case of the two wells, we measure the energies from the bottom of the e1 or hh1 band of well 2. More importantly,  $\nu_e^{(1)}$  and  $\nu_h^{(1)}$  depend on the material characteristics and can be orders of magnitude different. If  $\nu_e^{(1)} \ll \nu_h^{(1)}$ , the effective mass difference between electrons and holes can be overcompensated by the difference in the surface densities, and holes can tunnel more effectively than electrons do. This is the case, for instance, at the GaAs-oxide interface [8, 18]. In this case holes accumulate at the surface and in a steady-state situation  $p_1 > n_1$ . The electric field still given by equation (2) turns out to be negative.

As in the case of the two wells, the tunnelling current densities can be approximated by  $J_e = n_2/\tau_e$  and  $J_h = p_2/\tau_h$ . Now, however, we distinguish two cases. If  $n_1 > p_1$ , the tunnelling rates are given by equations (6)

and (7) with  $\nu_e^{(1)} = \nu_e^{(1)}(0)$  and  $\nu_h^{(1)} = \nu_h^{(1)}(0)$ . If  $p_1 > n_1$ , we have

$$\frac{1}{\tau_e} = \frac{2\pi}{\hbar} \left| \langle \Phi_0^{(1)} | V_c | \Phi_0^{(2)} \rangle \right|^2 A \nu_e^{(1)}(0) \quad (14)$$

$$\frac{1}{\tau_h} = \frac{2\pi}{\hbar} \left| \langle \Phi_0^{(1)} | V_b | \Phi_0^{(2)} \rangle \right|^2 A \nu_h^{(1)}(0) f \left( \frac{\epsilon_F^{(1)}}{k_B T} \right). \quad (15)$$

When the electric field and the tunnelling rates are known, the solution of the initial rate equations is still given by equation (8). With the conditions  $G_1 = 0$  and  $\lambda_1 \rightarrow \infty$  we get the simpler formulas

$$n_2 = \sqrt{\left( \frac{n}{2} + \frac{1}{2\lambda_2 \tau_e} \right)^2 + \frac{G_2}{\lambda_2}} - \left( \frac{n}{2} + \frac{1}{2\lambda_2 \tau_e} \right) \quad (16a)$$

$$n_1 = n \quad (16b)$$

$$p_1 = 0 \quad (16c)$$

$$p_2 = n_2 + n. \quad (16d)$$

The same recursive method as explained in section 2 allows us to find the steady-state values of the electric field, of the charge concentrations and of the tunnelling rates.

The evaluation of the luminescence intensity  $I_2$  implies the knowledge of the nature of the surface states. We can try to get information on the surface states by fitting experimental photoluminescence data. We will concentrate on the specific example of an  $\text{Al}_{0.3}\text{Ga}_{0.7}\text{As}$  surface with a nearby GaAs quantum well [1, 8]. At an energy close to the bottom of the e1 band of well 2 the  $\text{Al}_{0.3}\text{Ga}_{0.7}\text{As}$  surface has only donor-like states belonging to the exponentially vanishing Urbach tail:

$$\nu_e^{(1)}(\epsilon) = \frac{m_e^{(1)}}{\pi \hbar^2} \exp \left( - \frac{\Delta E_c + eFb - E_{e1}^{(2)} - \epsilon}{\epsilon_e} \right). \quad (17)$$

Such states are assumed to be nodal hydrogenic wavefunctions [19] with radius  $r_e$  fixed by the depth into the gap. Their explicit expression is given in appendix B. We assume that at the top of the gap the state density is the two-dimensional density of free  $\text{Al}_{0.3}\text{Ga}_{0.7}\text{As}$  electrons with effective mass  $m_e^{(1)}$ . The parameter  $\epsilon_e$  will be considered as a fitting parameter. According to equation (17) and equation (12) where we can assume  $E_{e1}^{(1)} = -\infty$ , the Fermi energy for the donor-like surface band is

$$\epsilon_F^{(1)} = \Delta E_c + eFb - E_{e1}^{(2)} + \epsilon_e \ln \left( \frac{\pi \hbar^2 n_1}{m_e^{(1)} \epsilon_e} \right). \quad (18)$$

On the other hand, at an energy close to the bottom of the hh1 band of well 2 the  $\text{Al}_{0.3}\text{Ga}_{0.7}\text{As}$  surface has a very high concentration of acceptor-like defect states [18]. We schematize them again by nodal hydrogenic wavefunctions [19] but with radius  $r_h$  to be considered as a second fitting parameter. These states are assumed to be distributed in energy with constant density  $\nu_h^{(1)}$ . The Fermi energy for the acceptor-like surface band is then

$$\epsilon_F^{(1)} = p_1/\nu_h^{(1)} + E_{hh1}^{(1)} + eFb - E_{hh1}^{(2)}. \quad (19)$$

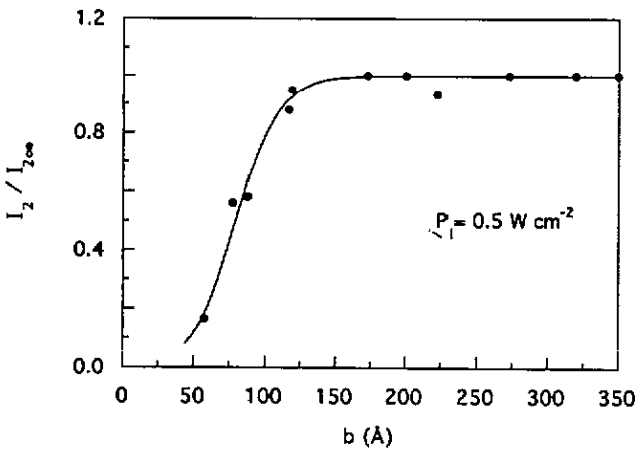


**Figure 5.** Normalized photoluminescence ratio  $I_2/I_{2\infty}$  of a near-surface well versus the surface barrier thickness  $b$ . Dots: experimental data from reference [1]; full curve: best fitting in terms of the self-consistent model. The incident power density is  $P_1 = 0.5 \text{ W cm}^{-2}$ .

The tunnelling matrix elements for the above surface states and surface densities are evaluated explicitly in appendix B.

According to the experiment reported in [1] we choose the well width  $a_2 = 60 \text{ \AA}$ , the temperature  $T = 4.2 \text{ K}$ , the photon energy  $h\nu = 1.608 \text{ eV}$  and the incident power density  $P_1 = 0.5 \text{ W cm}^{-2}$ . The incident efficiency is estimated to be 1% and we take  $G_2 = 0.01 P_1/h\nu$ . The relevant material parameters are [20]:  $\Delta E_c = 0.3 \text{ eV}$ ,  $\Delta E_v = 0.128 \text{ eV}$ ,  $m_e^{(1)} = 0.091m$ ,  $m_e^{(2)} = 0.067m$ ,  $m_h^{(2)} = 0.34m$ ,  $m$  being the free electron mass, and  $\epsilon_r = 12$ . Moreover we put  $\lambda_2 = 6 \text{ cm}^2 \text{ s}^{-1}$  [14]. We assume an acceptor-like surface state density  $v_h^{(1)} = 10^{14} \text{ cm}^{-2} \text{ eV}^{-1}$  [21] with  $E_{hh1}^{(1)} \simeq 1 \text{ eV}$  (the results we found do not depend crucially on this particular value). The free parameters,  $\epsilon_e$  and  $r_h$ , are fixed by fitting the normalized photoluminescence intensity  $I_2/I_{2\infty}$  to the experimental data [1] obtained for different values of the barrier width  $b$ . A least-square-error procedure gives the unique solution  $\epsilon_e = 12 \text{ meV}$  and  $r_h = 11 \text{ \AA}$ . In figure 5 a comparison is made between the ratio  $I_2/I_{2\infty}$ , calculated with these values, and the experimental data.

Because of the presence of two parameters the agreement between theoretical and experimental data in figure 5 should be considered as a source of information for these two parameters in the case when the model is valid rather than a proof of validity of the model itself. A reliable check of the validity of our model is obtained by comparing the theoretical values of the self-consistently estimated electric field  $F$  with the values deduced from measured Stark shifts as a function of the QW excitation [8]. The calculated field values are shown in figure 6 as a function of the barrier thickness  $b$ , for different values of the incident power. It is seen that, for high levels of excitation, the field approaches values of order  $10^5 \text{ V cm}^{-1}$  and keeps increasing when the barrier becomes thinner. Direct comparison with experiment is made for an  $80 \text{ \AA}$  thick barrier, a choice dictated by the wide laser power range where data were available for this moderately tunnelling sample. To obtain the value of the electric field

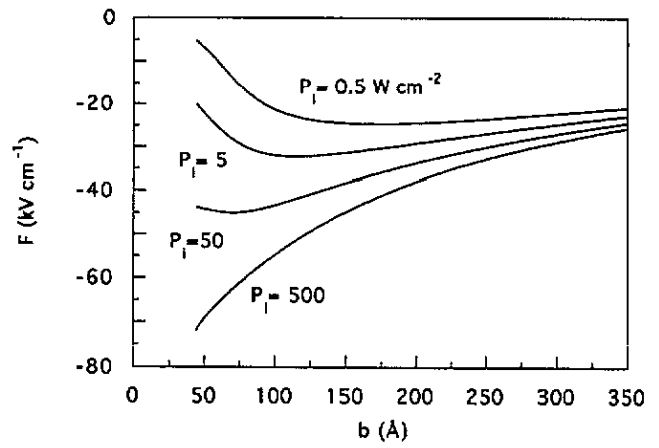


**Figure 6.** Calculated electric field  $F$  across the surface barrier versus the surface barrier thickness  $b$  for different incident power densities  $P_1$ .

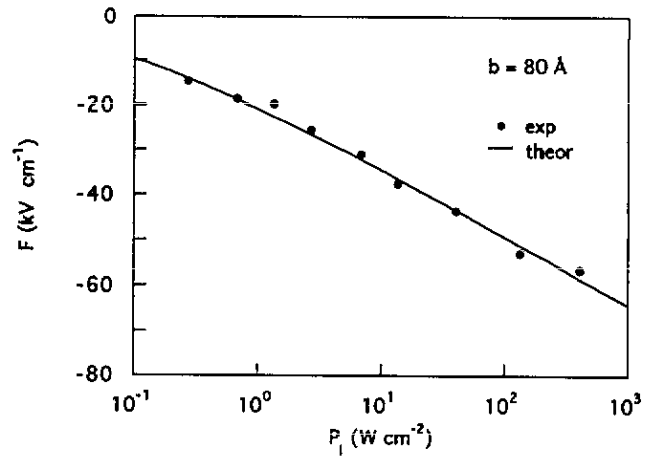


**Figure 7.** Comparison between the electric field  $F$  calculated from the model (full curve) and deduced from the measured Stark shifts [8] (dots) versus the incident power density  $P_1$ . The surface barrier thickness is  $b = 80 \text{ \AA}$ .

from the measured Stark shift  $\Delta E_p$  we use the relationship  $\Delta E_p = K F^{3/2}$ , empirically deduced from known results in the literature [22, 23]. The constant  $K$  is fixed by requiring that the electric field obtained from the measured Stark shift  $\Delta E_p = 0.33 \text{ meV}$ , corresponding to an incident power density  $P_1 = 0.68 \text{ W cm}^{-2}$ , coincides with the calculated value. We obtain  $K = 1.25 \times 10^{-7} \text{ meV (V cm}^{-1})^{-3/2}$ , which compares well with the values extracted from the data of reference [22],  $K \simeq 1 \times 10^{-7} \text{ meV (V cm}^{-1})^{-3/2}$ , and reference [23],  $K \simeq 0.6 \times 10^{-7} \text{ meV (V cm}^{-1})^{-3/2}$ .

The comparison between the calculated and experimentally deduced electric fields is shown in figure 7 as a function of the incident power density. The agreement is very good for a power range extending over three orders of magnitude. The near-coincidence of the scale factor  $K$  with other independently obtained values should not be attributed much importance, on one hand because of the approximations used in the model, e.g. density and distribution of surface states, and on the other hand because the experimental Stark shift is observed in the luminescence from the quantum well, where the field is non-uniform and possibly different from its value in the barrier [8]. Instead,

the correct functional dependence of the field on the excitation level is a clear confirmation that the self-consistent approach provides a reasonably accurate description of the whole process.

#### 4. Conclusions

The photoluminescence efficiency in asymmetric double quantum wells and in near-surface quantum wells is strongly influenced by the tunnelling of both electrons and holes between the two wells, or the well and the surface states. The theoretical model presented here takes into account this effect and allows a quantitative prediction for the photoluminescence rates and the value of the electric field which needs to be established across the tunnelling barrier in a steady-state situation. Experimental results regarding both ADQW and near-surface QWs, namely changes in photoluminescence efficiency and peak shifts due to the self-induced electric field, are very well accounted for.

Our model can be readily generalized to include the case of an externally applied electric field as well as the case of excitation that is not constant.

#### Acknowledgments

We thank M Capizzi, B Bonanni and M Colocci for very profitable discussions.

#### Appendix A. ADQW matrix elements

We call  $z$  the coordinate orthogonal to the interfaces and suppose that the quantum well 1 is in  $-a_1 \leq z \leq 0$  and the quantum well 2 in  $b \leq z \leq b + a_2$ . Firstly let us consider the case of electrons. As schematized in figure 8 we assume a rectangular potential profile with left and right discontinuities  $V_l^{(1)} = \Delta E_c$  and  $V_r^{(1)} = \Delta E_c - eFb/2$  for well 1 and  $V_l^{(2)} = \Delta E_c + eFb/2$  and  $V_r^{(2)} = \Delta E_c$  for well 2 where  $F$  is the electric field in the barrier region  $0 \leq z \leq b$ . The electron wavefunctions at energy  $\epsilon$ , measured from the bottom of the e1 band of well 2, are

$$\Phi_\epsilon^{(1)}(x, y, z) = \frac{\exp(ik_x^{(1)}x + ik_y^{(1)}y)}{\sqrt{A}} C^{(1)} \times \begin{cases} \sin \delta^{(1)} e^{k_l^{(1)}(z+a_1)} & z < -a_1 \\ \sin[k^{(1)}(z+a_1) + \delta^{(1)}] & -a_1 < z < 0 \\ \sin(k^{(1)}a_1 + \delta^{(1)}) e^{-k_r^{(1)}z} & 0 < z \end{cases} \quad (\text{A1})$$

where

$$\frac{\hbar^2}{2m_e^{(1)}} [(k_x^{(1)})^2 + (k_y^{(1)})^2] = \epsilon + E_{e1}^{(2)} - E_{e1}^{(1)} - eFb \quad (\text{A2})$$

$$k_l^{(1)} = \sqrt{\frac{2m_e^{(1)}}{\hbar^2} (\Delta E_c - E_{e1}^{(1)})} \quad (\text{A3})$$

$$k^{(1)} = \sqrt{\frac{2m_e^{(1)}}{\hbar^2} E_{e1}^{(1)}} \quad (\text{A4})$$

$$k_r^{(1)} = \sqrt{\frac{2m_e^{(1)}}{\hbar^2} (\Delta E_c - eFb/2 - E_{e1}^{(1)})} \quad (\text{A5})$$

for well 1 and

$$\Phi_\epsilon^{(2)}(x, y, z) = \frac{\exp(ik_x^{(2)}x + ik_y^{(2)}y)}{\sqrt{A}} C^{(2)} \times \begin{cases} \sin \delta^{(2)} e^{k_l^{(2)}(z-b)} & z < b \\ \sin[k^{(2)}(z-b) + \delta^{(2)}] & b < z < b + a_2 \\ \sin(k^{(2)}a_2 + \delta^{(2)}) e^{-k_r^{(2)}(z-b-a_2)} & b + a_2 < z \end{cases} \quad (\text{A6})$$

where

$$\frac{\hbar^2}{2m_e^{(2)}} [(k_x^{(2)})^2 + (k_y^{(2)})^2] = \epsilon \quad (\text{A7})$$

$$k_l^{(2)} = \sqrt{\frac{2m_e^{(2)}}{\hbar^2} (\Delta E_c + eFb/2 - E_{e1}^{(2)})} \quad (\text{A8})$$

$$k^{(2)} = \sqrt{\frac{2m_e^{(2)}}{\hbar^2} E_{e1}^{(2)}} \quad (\text{A9})$$

$$k_r^{(2)} = \sqrt{\frac{2m_e^{(2)}}{\hbar^2} (\Delta E_c - E_{e1}^{(2)})} \quad (\text{A10})$$

for well 2. The energy  $E_{e1}^{(i)}$  measures the bottom of the e1 band in the well  $i = 1, 2$  from the bottom of that well and is determined by solving

$$k^{(i)}a_i = \pi - \sin^{-1} \left( \frac{\hbar k^{(i)}}{\sqrt{2m_e^{(i)} V_l^{(i)}}} \right) - \sin^{-1} \left( \frac{\hbar k^{(i)}}{\sqrt{2m_e^{(i)} V_r^{(i)}}} \right). \quad (\text{A11})$$

The phase shifts are  $\delta^{(i)} = \tan^{-1}(k^{(i)}/k_l^{(i)})$ ,  $i = 1, 2$ . The constants  $C^{(i)}$ ,  $i = 1, 2$ , are fixed by normalizing the wavefunctions  $\Phi_\epsilon^{(i)}$ :

$$C^{(i)} = \left( \frac{\sin^2 \delta^{(i)}}{2k_l^{(i)}} + \frac{\sin^2(k^{(i)}a_i + \delta^{(i)})}{2k_r^{(i)}} + \frac{a_i}{2} - \frac{\sin[2(k^{(i)}a_i + \delta^{(i)})] - \sin(2\delta^{(i)})}{4k^{(i)}} \right)^{-1/2}. \quad (\text{A12})$$

For  $\epsilon = 0$  and with the assumption that  $V_e$  in equation (6) vanishes everywhere but in the barrier region where  $V_e = \Delta E_c$ , the tunnelling matrix element is

$$\begin{aligned} & \langle \Phi_0^{(1)} | V_e | \Phi_0^{(2)} \rangle \\ &= \int_0^{\sqrt{A}} dx \int_0^{\sqrt{A}} dy \int_0^b dz \frac{\exp(-ik_x^{(1)}x - ik_y^{(1)}y)}{\sqrt{A}} \\ & \quad \times C^{(1)} \sin(k^{(1)}a_1 + \delta^{(1)}) e^{-k_r^{(1)}z} \Delta E_c \frac{1}{\sqrt{A}} \\ & \quad \times C^{(2)} \sin \delta^{(2)} e^{k_l^{(2)}(z-b)} \\ &= \frac{C^{(1)} C^{(2)}}{A} \sin(k^{(1)}a_1 + \delta^{(1)}) \sin \delta^{(2)} \\ & \quad \times \frac{e^{-k_r^{(1)}b} - e^{-k_r^{(2)}b}}{k_l^{(2)} - k_r^{(1)}} \frac{1 - e^{-ik_x^{(1)}\sqrt{A}}}{ik_x^{(1)}} \frac{1 - e^{-ik_y^{(1)}\sqrt{A}}}{ik_y^{(1)}}. \end{aligned} \quad (\text{A13})$$

The last two factors in (A.13) oscillate quickly with  $k_x^{(1)}$  and  $k_y^{(1)}$  ( $k_x^{(1)}$ ) =  $\sqrt{2m_e^{(1)}(E_{e1}^{(2)} - E_{e1}^{(1)} - eFb)/\hbar^2 - (k_x^{(1)})^2}$ .

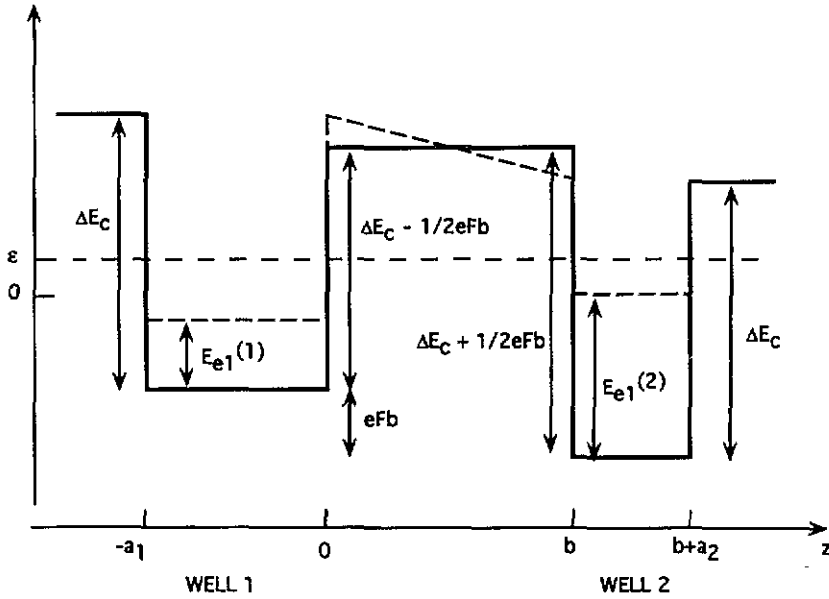


Figure 8. Energy-space diagram for electrons in the asymmetric double quantum well.

By taking the value for  $k_x^{(1)} = 0$  (maximum value) the electron tunnelling matrix element is estimated as

$$\begin{aligned} & \left| \langle \Phi_0^{(1)} | V_c | \Phi_0^{(2)} \rangle \right| \\ & \simeq \left| \frac{2\hbar \Delta E_c C^{(1)} C^{(2)} \sin(k^{(1)} a_1 + \delta^{(1)}) \sin \delta^{(2)}}{\sqrt{2m_e^{(1)} A(E_{e1}^{(2)} - E_{e1}^{(1)} - eFb)}} \right. \\ & \quad \left. \times \frac{e^{-k_r^{(1)} b} - e^{-k_r^{(2)} b}}{k_r^{(2)} - k_r^{(1)}} \right|. \end{aligned} \quad (A14)$$

In the case of holes we have a completely analogous situation where the relevant band is hh1 instead of e1. The expressions derived for electrons still hold for holes with the substitutions  $m_e^{(i)} \rightarrow m_h^{(i)}$ ,  $i = 1, 2$ ,  $\Delta E_c \rightarrow \Delta E_v$ ,  $eFb \rightarrow -eFb$ .

### Appendix B. Near-surface qw matrix elements

Following the notation of appendix A, the surface is defined by the plane  $z = 0$  and well 2 is in  $b < z < b + a_2$ . Firstly, we consider the case of electrons and we measure the energy from the bottom of the e1 band of well 2. The state  $\Phi_\epsilon^{(2)}(x, y, z)$  is given by equation (A6). The donor-like surface state  $\Phi_\epsilon^{(1)}(x, y, z)$  is approximated by a truncated 2p hydrogenic wavefunction [19]:

$$\Phi_\epsilon^{(1)}(x, y, z) = \frac{z}{4\sqrt{\pi} r_e^{5/2}} e^{r/2r_e} \begin{cases} 0 & z < 0 \\ 1 & 0 < z \end{cases} \quad (B1)$$

where  $r = \sqrt{x^2 + y^2 + z^2}$ . The state is at an energy  $\hbar^2/8m_e^{(1)}r_e^2$  below the bottom of the conduction band for the barrier material where the electron effective mass is  $m_e^{(1)}$ . By requiring this energy to correspond to  $\epsilon$  we determine the radius  $r_e$ ,

$$r_e = \frac{\hbar}{\sqrt{8m_e^{(1)} (\Delta E_c - E_{e1}^{(2)} + eFb - \epsilon)}}. \quad (B2)$$

Using parabolic coordinates  $\eta = (r - z)/r_e$ ,  $\xi = (r + z)/r_e$ ,  $\varphi = \tan^{-1}(y/x)$ , the tunnelling matrix element between the well and surface states at  $\epsilon = 0$  is

$$\begin{aligned} & \langle \Phi_0^{(1)} | V_c | \Phi_0^{(2)} \rangle \\ & = \int_0^\infty d\eta \int_\eta^{\eta+2b/r_e} d\xi \int_0^{2\pi} d\varphi \frac{r_e^3 (\xi + \eta)}{4} \\ & \quad \times \frac{(\xi - \eta) e^{-(\xi+\eta)/4}}{8\sqrt{\pi} r_e^{3/2}} \frac{\Delta E_c C^{(2)} \sin \delta^{(2)} e^{k_i^{(2)} ((\xi - \eta)r_e/2 - b)}}{\sqrt{A}} \\ & = \frac{\sqrt{\pi} r_e^{3/2} \Delta E_c C^{(2)} \sin \delta^{(2)}}{8\sqrt{A}} \\ & \quad \times \left[ e^{-k_i^{(2)} b} \left( \frac{1}{4(2k_i^{(2)} r_e - 1)^2} - \frac{1}{32(2k_i^{(2)} r_e - 1)^3} \right) \right. \\ & \quad + e^{-b/2r_e} \left( \frac{(b/r_e)^2 + 2b/r_e}{2k_i^{(2)} r_e - 1} - \frac{1 + b/r_e}{4(2k_i^{(2)} r_e - 1)^2} \right. \\ & \quad \left. \left. + \frac{1}{32(2k_i^{(2)} r_e - 1)^3} \right) \right]. \end{aligned} \quad (B3)$$

In the case of holes we have a completely analogous situation where the relevant band of well 2 is hh1 instead of e1 and the acceptor-like surface state is given by equation (B1) with  $r_e \rightarrow r_h$ . Equation (B3) gives the tunnelling matrix element for holes with the substitutions  $r_e \rightarrow r_h$ ,  $\Delta E_c \rightarrow \Delta E_v$ ,  $eFb \rightarrow -eFb$ .

### References

- [1] Chang Y L, Tan I H, Zhang Y H, Merz J, Hu E, Frova A and Emiliani V 1993 *Appl. Phys. Lett.* **62** 2697
- [2] Moison J M, Elcess K, Houzay F, Marzin J Y, Gerard J M, Barthe F and Bensoussan M 1990 *Phys. Rev. B* **41** 12945
- [3] Sobiesierski Z, Westwood D I, Fujikura H, Fukui T and Hasegawa H 1993 *J. Vac. Sci. Technol. B* **11** 7010
- [4] Astratov V N and Vlasov Yu A 1993 *Proc. ICDS-17 Conf., 18-23 July 1993, Gmunden (Austria)*

- [5] Norris T B, Vodjdani N, Vinter B, Costard E and Böckenhoff E 1991 *Phys. Rev. B* **43** 1867
- [6] Capasso F, Mohammed K, Cho A Y, Hull R and Hutchinson A L 1985 *Appl. Phys. Lett.* **47** 420
- [7] Nido M, Alexander M G, Rühle W W, Schweizer T and Köhler K 1990 *Appl. Phys. Lett.* **56** 355
- [8] Emiliani V, Bonanni B, Presilla C, Capizzi M, Frova A, Chang Y L, Tan I H, Merz J L, Colocci M and Gurioli M 1994 *J. Appl. Phys.* **75** 5114
- [9] Sauer R, Thonke K and Tsang W T 1988 *Phys. Rev. Lett.* **61** 609
- [10] Roussignol Ph, Vinattieri A, Carraresi L, Colocci M and Fasolino A 1991 *Phys. Rev. B* **44** 8873
- [11] Colocci M, Gurioli M, Vinattieri A, Fermi F, Deporis C, Massaies J and Neu G 1991 *Europhys. Lett.* **12** 417
- [12] Miller D A B, Chemla D S, Damen T C, Gossard A C, Wiegmann W, Wood T H and Burrus C A 1984 *Phys. Rev. Lett.* **53** 2173
- [13] Ferreira R, Rolland P, Roussignol Ph, Delande C, Vinattieri A, Carraresi L, Colocci M, Roy N, Sermage B, Palmier J F and Etienne B 1992 *Phys. Rev. B* **45** 11782
- [14] Strobel R, Eccleston R, Kuhl J and Köhler K 1991 *Phys. Rev. B* **43** 12564
- [15] Nagarajan R, Ishikawa M, Fukushima T, Geels R S and Bowers J E 1992 *IEEE J. Quantum Electron.* **28** 1990
- [16] Landau L D and Lifshits E M 1958 *Quantum Mechanics, Nonrelativistic Theory* (Oxford: Pergamon)
- [17] Landolt-Börnstein 1982 *Numerical Data and Functional Relationships in Science and Technology* vol 17 ed O Madelung *et al* (Berlin: Springer)
- [18] Spicer W E, Liliental-Weber Z, Weber E, Newman N, Kendelewicz T, Cao R, McCants C, Mahowald P, Miyano K and Lindau I 1988 *J. Vac. Sci. Technol. B* **6** 1245
- [19] Levine J D 1965 *Phys. Rev.* **140** 586
- [20] Atanasov R and Bassani F 1992 *Solid State Commun.* **84** 71
- [21] Spicer W E, Chye P W, Skeath P R, Su C Y and Lindau I 1979 *J. Vac. Sci. Technol.* **16** 1422
- [22] Goebel E O 1988 *Springer Proceedings in Physics* vol 25 (Berlin: Springer) pp 204–17
- [23] Viña L, Collins R T, Mendez E E, Chang L L and Esaki L 1988 *Springer Proceedings in Physics* vol 25 (Berlin: Springer) pp 230–43